Aerospace Technology Congress, 8-9 October 2019, Stockholm, Sweden
Swedish Society of Aeronautics and Astronautics (FTF)

Equations of State in Fighter Aircraft Oleo-pneumatic Shock Absorber Modelling

Arttu Heininen , Jussi Aaltonen , Kari T. Koskinen , and Juha Huitula*

Automation Technology and Mechanical Engineering, Tampere University, Tampere, Finland
E-mail: arttu.heininen@tuni.fi, jussi.aaltonen@tuni.fi, kari.koskinen@tuni.fi, juha.huitula@mil.fi
*Finnish Defense Forces Logistics Command, Tampere, Finland

Abstract

Most of all modern commercial and military aircraft have oleo-pneumatic shock absorbers in their landing gear. An oleo-pneumatic shock absorber consists of a gas charge and an oil fill. During the stroke oil is forced through orifices which provides damping, while the gas charge is compressed and acts as a spring by increasing the stiffness of the shock absorber. Typically, when the gas behaviour is modelled, the ideal gas law is used as the equation of state as this provides in most cases adequate fidelity with relatively light computational load. However, in a fighter aircraft, especially in naval service, the gas pressure inside a shock absorber raises too high during landing for the ideal gas assumption to be valid. Therefore, other well-established equations of state have been considered. These are Van der Waals, Redlich-Kwong-Soave, and Peng-Robinson equation of state. This paper presents a multi-physics simulation model of a two-chamber oleo-pneumatic shock absorber based on fundamental analytical equations. Using this model, the behaviour of the aforementioned equations of state are studied in two cases: quasi-static and dynamical compression. The simulation results are compared to laboratory measurements. This comparison verifies that the ideal gas law should not be used when modelling naval fighter aircraft shock absorbers.
Keywords: Fighter aircraft, Shock absorber, Modelling, Simulation

1 Introduction

Essentially every modern aircraft, military or civilian, has some kind of landing gear. While there are many different landing gear configurations, most of them have a shock absorber to dissipate the kinetic energy related to landing.

Typically, shock absorber are either using a solid spring made of steel or rubber or a fluid spring. Solid spring shock absorbers are used in light aircraft and fluid springs in heavier aircraft. The most common shock absorber type is an oleo-pneumatic shock absorber. These have a high damping to weight ratio and are used in most modern fighter aircraft. An oleo-pneumatic shock absorber has both a gas charge, typically nitrogen or dry air is used, and a hydraulic oil fill. [1]

The gas charge acts as a spring when compressed. Becoming stiffer as the compression continues. Depending on the initial charge pressure, and the amount of gas and the stroke, the pressure increase can be very high. Especially in the case of naval fighter aircraft, because of their high sink speed during landing.

Usually, when modelling these shock absorbers using fundamental analytical equations, the gas and liquid volumes are modelled separately as control volumes. These can exchange mass and heat between control volumes that has the same substance, i.e., nitrogen or hydraulic oil. Between different substance control volumes only heat is transferred.

There are two ways to model the thermal behaviour of the gas control volumes. The first method is to model the gas compression as a polytropic process. This method depends on the chosen polytropic constant. For a slow rate of compression the polytropic constant approaches 1.0, which would indicate a isothermal process; whereas higher rates approach adiabatic process and a value of 1.4 for the constant could be used. Typically, if the gas and oil are separated, value of 1.35 is found to give accurate results, and 1.1 if the gas and oil is mixed. [1], [2]

Second method to model the gas is to use general internal energy model that is based on the first law of thermodynamics. This is a more accurate method, as in the first method the thermal exchange is only represented by one constant, and as such is a simple model.

The thermal behaviour of a gas volume based on the internal energy model uses a gas *equation of state* (EOS) to define the density and its derivatives. Therefore, the chosen *EOS* affects the predicted pressure and stiffness of the shock absorber. One of the simplest *EOS* is the ideal gas assumption. However, models based on this assumption behave poorly in high pressures [3]. For this reason, it is assumed that using the ideal gas assumption, when modelling a naval fighter aircraft shock absorber, produces poor results.

A schematic view of a naval fighter aircraft shock absorber is shown in fig. 1. It is a two-stage oleo-pneumatic shock

DOI
10.3384/ecp19162007

absorber, meaning that there are two chambers: primary and secondary chamber. The primary chamber is filled with gas and oil, just like a conventional oleo-pneumatic shock absorber, while the secondary chamber is filled with high pressure gas only.

As the shock absorber is compressed, the oil is forced from the bottom part of the primary chamber to the upper part through an orifice that is controlled with a metering pin, which has a variable cross-section. It is typically modelled using orifice flow model with a stroke dependent cross-section ([4], [5]). This approach is also used in this paper.

If the stroke is long enough, the primary chamber hits end-stops and the secondary chamber is engaged. The secondary chamber has a high stiffness due to the high pressure. Therefore, a rapid increase in the force is required for the shock absorber to further compress.

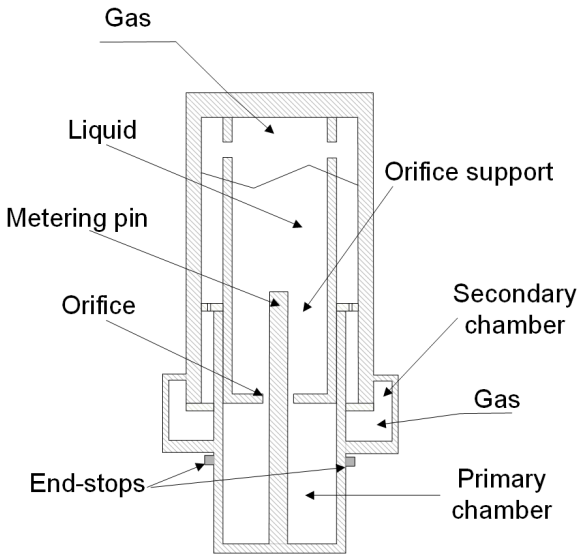

Figure 1: A schematic view of a two-stage oleo-pneumatic shock absorber.

The model presented in this paper is based on the aforementioned control volume approach. The gas volumes has been modelled using the general internal energy model using different *EOS*. These are the ideal gas assumption, Van der Waals, Redlich-Kwong-Soave, and Peng-Robinson *EOS*. Using the model two different cases are considered: quasi-static compression and dynamic compression. Both cases are simulated using the shock absorber model and the results are compared to those acquired by laboratory measurements. The aim of the measurements were to discover any abnormal behaviour and to provide more detailed information how the shock absorber behaves under different conditions. The aim of this paper is to provide a shock absorber model based on the internal energy model. The aim of this paper is to present a naval fighter aircraft shock absorber model based on fundamental analytical equations using the internal energy model. In the model, different *EOS* are considered, and it is shown that the pressure inside the shock absorber rises so high that the ideal gas law becomes inaccurate. Therefore, more accurate *EOS* should be used.

2 The shock absorber model

Balancing the forces that affect the moving parts of the shock absorber yields the following equation

$$\begin{aligned} F_{sa} = m_{sa}g - p_u A_{mp} - p_L(A_L - A_{mp}) \\ -A_{ph}(p_u - p_{ph}) - A_{HP}p_{HP} - F_{\mu 1} - F_{\mu 2} - F_{\mu 3}. \end{aligned} \tag{1}$$

To solve this equation, the pressure must be solved inside the primary chamber, orifice support and secondary chamber. In addition, there are several sources for friction: friction of the primary chamber, viscous friction of the main cylinder and the friction of the secondary chamber. These must also be modelled. Figure 2 shows the pressure and friction sources inside the shock absorber. Due to the limited length, this paper only covers the most important parts of the model. A more detailed explanation of the model can be found in [6].

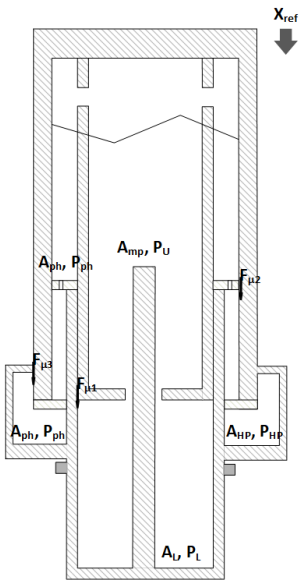

Figure 2: Pressure and friction sources inside the shock absorber.

2.1 Liquid volumes

The model is based on connected thermal-hydraulic and gas volumes together that exchange heat with each other. No mass is transferred between the two phases.

Considering a volume of liquid, its density is a function of pressure and temperature. Differentiating this we get

$$d\rho = \left(\frac{\partial \rho}{\partial p}\right)_T dp + \left(\frac{\partial \rho}{\partial T}\right)_p dT \tag{2}$$

Solving for dp and taking its time derivative yields

$$\frac{dp}{dt} = \frac{1}{\left(\frac{\partial \rho}{\partial p}\right)_T}\left[d\rho - \left(\frac{\partial \rho}{\partial T}\right)_P dT\right]. \tag{3}$$

The isothermal bulk modulus of a liquid is

$$\beta_T(p,T) = \frac{\rho}{\left(\frac{\partial\rho}{\partial p}\right)_T} \tag{4}$$

and

$$\alpha_P(p,T) = -\frac{1}{\rho}\left(\frac{\partial\rho}{\partial T}\right)_p \tag{5}$$

is the volumetric expansion coefficient.

The continuity equation is

$$\frac{dm}{dt} = V\frac{d\rho}{dt} + \rho\frac{dV}{dt} \tag{6}$$

and solving for $d\rho/dt$ we get

$$\frac{d\rho}{dt} = \frac{\frac{dm}{dt} - \rho\frac{dV}{dt}}{V} \tag{7}$$

Combining equations 4, 5, and 7 with 3, the pressure change in a volume liquid is

$$\frac{dp}{dt} = \beta_T\left[\frac{1}{\rho V}\left(\frac{dm}{dt} - \rho\frac{dV}{dt}\right) + \alpha_p\frac{dT}{dt}\right]. \tag{8}$$

The change in the total energy of the volume, neglecting the kinetic and potential energies, is

$$dE = d(mu) = mdu + udm \tag{9}$$

where the change in the specific internal energy is

$$du = dh - \frac{dp}{\rho} \tag{10}$$

and in the specific enthalpy

$$\begin{aligned} dh = \left(\frac{\partial h}{\partial T}\right)_P dT + \left(\frac{\partial h}{\partial P}\right)_T dP = \\ c_P dT + (1-\alpha T)\frac{1}{\rho}dP \end{aligned} \tag{11}$$

so the change in the internal specific energy becomes

$$du = c_P dT - \frac{\alpha T}{\rho}dP \tag{12}$$

and the change in the total energy

$$dE = (h - \frac{P}{\rho})dm + mc_P dT - \frac{m\alpha T}{\rho}dP. \tag{13}$$

Now the change in the total energy is equal to the heat exchange with the volume's surroundings

$$dE = dQ. \tag{14}$$

Combining equations 9 and 14 and taking time derivative yields

$$\frac{dT}{dt} = \frac{\dot{Q} + (\frac{P}{\rho} - h)\dot{m}}{mc_P} + \frac{\alpha T}{c_P\rho}\frac{dP}{dt} \tag{15}$$

2.2 Gas volumes

Considering a gas volume, its rate of change of mass can be written

$$\frac{dm}{dt} = \rho\frac{dV}{dt} + V\left[\left(\frac{\partial\rho}{\partial P}\right)_T\frac{dP}{dt} + \left(\frac{\partial\rho}{\partial T}\right)_P\frac{dT}{dt}\right]. \tag{16}$$

Considering the same gas volume, its internal energy is

$$U = mu \tag{17}$$

and its total derivative is

$$dU = d(mu) = dmu + mdu. \tag{18}$$

Using the internal energy, the specific enthalpy of the gas volume is

$$h = u + Pv \tag{19}$$

and substituting this in equation 18 yields

$$\begin{aligned} dU &= dm(h-Pv) + md(h-Pv) \\ &= dm(v-Pv) + mdh + m(-dPv - Pdv) \\ &= dmh - dmPv + mdh - mPdv - mvdP \\ &= dmh - dmPv + mdh - mPdv - Vdp \\ &= dmh + mdh - VdP - Pd(mv) \\ &= dmh + mdh - VdP - PdV. \end{aligned} \tag{20}$$

On the other hand, using the first law of thermodynamics, the change in internal energy can be written as

$$dU = hdm + \delta Q + dW \tag{21}$$

where the work done by the system is

$$dW = -PdV \tag{22}$$

Combining equations 17 and 23 we get

$$\sum_i m_i h_i - \sum_i m_i h + \delta Q = mdh - VdP \tag{23}$$

Taking a time derivative of the above equation and considering the *state postulate* we have

$$\left(m\left(\frac{\partial h}{\partial P}\right)_T - V\right)\frac{dP}{dt} + m\left(\frac{\partial h}{\partial T}\right)_P \frac{dT}{dt} = \sum_i \frac{dm_i}{dt}h_i - \sum_i \frac{dm_i}{dt}h + \delta Q \tag{24}$$

Now we can form a system of equation using equations

$$\begin{bmatrix} V\left(\frac{\partial \rho}{\partial P}\right)_T & V\left(\frac{\partial \rho}{\partial T}\right)_P \\ m\left(\frac{\partial h}{\partial P}\right)_T - V & m\left(\frac{\partial h}{\partial T}\right)_P \end{bmatrix} \begin{bmatrix} \frac{\partial P}{dt} \\ \frac{dT}{dt} \end{bmatrix} = \begin{bmatrix} \sum_i \frac{dm_i}{dt} - \rho\frac{dV}{dt} \\ \sum_i \frac{dm_i}{dt}h_i - h\sum_i \frac{dm_i}{dt} + \delta Q \end{bmatrix} \tag{25}$$

Finally, the derivatives of ρ are solved from the chosen equation of state.

2.3 Equations of state

The most simple way to model the gas behaviour is to use the ideal gas law:

$$PV = mrT. \tag{26}$$

Most of the real gases in mild temperatures or pressures behave like an ideal gas. However, it does not consider the volume that the gas molecules occupy or the intermolecular attraction forces. Therefore, its ability to accurately predict the gas state decreases as the gas pressure rises.

To take the interaction of the gas molecules into consideration van der Waals proposed an equation of state [7]

$$(P + \frac{a}{V^2})(V - b) - rT = 0. \tag{27}$$

where

$$a = \frac{27r^2T_c^2}{64P_c} \tag{28}$$

and

$$b = \frac{rT_c}{8P_c} \tag{29}$$

Even though van der Waals *EOS* is an improvement over the ideal gas law, several more accurate *EOS* have been proposed after its publication. However, most of these, like Redlich-Kwong-Soave and Peng-Robinson *EOS* are based on the van der Waals *EOS*. So similar behaviour can be assumed.

Soave [8] proposed an *EOS* based on the works of Redlich and Kwong [9]. The main difference of these models is that the constant a has been replaced with a more general temperature dependent product of $a\alpha(T)$. It is similar to van der Waals equation but with some modifications:

$$(P + \frac{a\alpha(T)}{V(V+b)})(V - b) - rT = 0 \tag{30}$$

where

$$a = 0.42748024\frac{r^2T_c^2}{P_c} \tag{31}$$

and

$$b = 0.08664035\frac{rT_c}{P_c} \tag{32}$$

and the temperature dependent adimensional factor α

$$\alpha(T) = \left[1 + m\left(1 - \sqrt{\frac{T}{T_c}}\right)\right]^2 \tag{33}$$

where m is a substance dependent constant

$$m = 0.48 + 1.574\omega - 0.176\omega^2 \tag{34}$$

defined by the acentric factor ω

$$\omega = -1 - 1log_{10}\left(\frac{P_{sat}}{P_c}\right)_{T=0.7T_c}. \tag{35}$$

Peng and Robinson noticed that the Redlich-Kwong-Soave *EOS* predicted greater specific volumes than found in the literature [10]. To correct this behaviour, they proposed an *EOS* similar to Redlich-Kwong-Soave:

$$\left(P + \frac{a\alpha(T)}{V^2 + 2bV - b^2}\right)(V - b) - rT = 0. \tag{36}$$

Here the adimensional factor α(T) is the same as in Redlich-Kwong-Soave EOS, but m has a different constants in it

$$m = 0.37464 + 1.54226\omega - 0.26992\omega^2. \tag{37}$$

According to literature, Peng-Robinson *EOS* should be the most accurate of the two-constant *EOS* presented here. [10]

2.4 Friction model

Friction can be modelled using plethora of different friction models [11]. Here, a widely applied Karnopp friction model is used ([11], [12]) to model the friction between the orifice support and the secondary chamber, $F_{\mu 3}$:

$$F_{\mu 3} = \begin{cases} min(|F_E|, |F_S|)sign(F_E) \quad \text{and} \quad v = 0 \quad if|v| < dv \\ (F_C + (F_S - F_C)e^{-3|v|/V_S})sign(v) + F_V V \ if|v| > dv \end{cases} \tag{38}$$

2.5 End-stops

The viscous friction of the main cylinder, $F_{\mu 2}$ is modelled as a moving cylinder within an envelope. It is based on the Karnopp friction model, equation 38, but also considers the viscous friction and the elastic end-stops.

The friction force between the cylinder and envelope is:

$$F_{\mu 2} = \frac{m_1 f_2 - m_2 f_1}{m_1 + m_2} \tag{39}$$

where

$$f_1 = F_{ext1} - F_{ext2} + F_{min} - F_{max} + F_{min3} - F_{max3} + m_1 g - R_{visc} V_{rel} \tag{40}$$

and

$$f_2 = F_{ext3} - F_{ext4} - F_{min} + F_{max} + F_{min2} - F_{max2} + m_2 g - R_{visc} V_{rel}. \tag{41}$$

The contact forces at the lower limit is F_{min}, F_{min2}, and F_{min3} are calculated from

$$F_{min} = Kb_{min}(X_{min} - X_{rel}) - Db_{min}\left(1 - e^{\frac{-(X_{min} - Xrel)}{Pd_{min}}}\right) V_{rel} \tag{42}$$

if X_{rel} is smaller than the lower displacement limit and zero otherwise. The contact forces at the higher limit is:

$$F_{max} = Kb_{max}(X_{rel} - X_{max}) - Db_{max}\left(1 - e^{\frac{-(X_{rel} - Xmax)}{Pd_{max}}}\right) V_{rel} \tag{43}$$

and zero if $X_{rel} \leq X_{max}$.

2.6 Orifice flow

A flow through an orifice can be described by

$$\dot{m} = \rho c_q A \sqrt{\frac{2|\Delta P|}{\rho}} \tag{44}$$

where A is the area of the orifice subtracted by the area of the metering pin.

3 Numerical solution

The aforementioned equations were modelled using a commercial multi-domain simulation software LMS Imagine.Lab Amesim 15, which uses bond graphs to represent systems. The software has many well-known algorithms to solve ordinary differential equations, based on linear multi-step methods.

4 Validation

The model was used to simulate two different cases: quasi-static and dynamic compression. In the quasi-static case, the shock absorber is compressed so slowly that the hydraulic damping is negligible, while the dynamic case considers damping also. In both cases simulation results are compared to the actual measured data.

4.1 Quasi-static case

The test setup of the quasi-static case has a hydraulic cylinder that is attached to the end of the shock absorber. The other end is rigidly supported preventing its movement. The motion of the hydraulic cylinder is controlled using PID-controller, so that the compression is the same during each individual test.

The pressure is measured in the hydraulic cylinder during the test and the compression force is calculated from this pressure. The test system then produces a graph with the force as a function of the shock absorber stroke. The stroke, as an function of time, is given as an input to the model presented in this paper. The given input normalised with the maximum shock absorber design stroke is shown in 3.

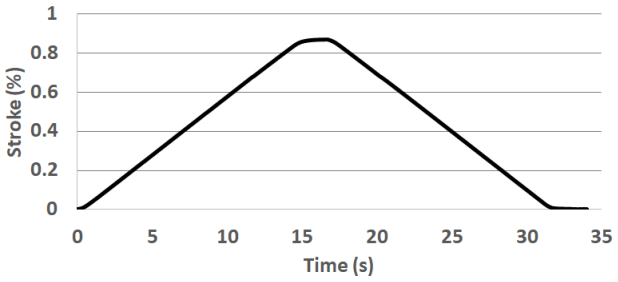

Figure 3: The stroke data given as in input to the model in the quasi-static case.

The force predicted by the model and the measured force is shown in fig. 4. The stroke-force plot is divided into two distinguishable parts. First, there is the initial part, where the primary chamber is compressed. This is followed by the secondary part, where the secondary chamber also activates. Between these two parts there is a vertical line. The secondary chamber has an initial stiffness and requires a certain force, before it activates.

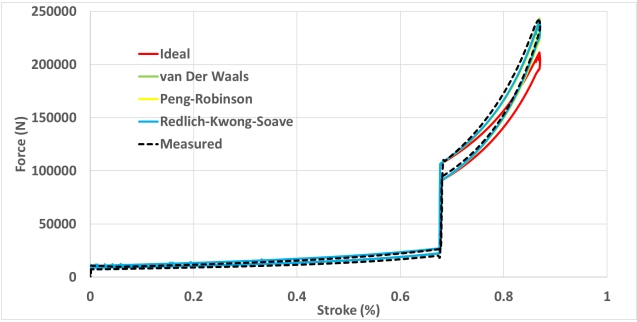

Figure 4: Force-stroke curve during quasi-static compression.

Figure 4 clearly shows that the force predicted using the ideal gas law is poor compared to the measurements. This is apparent, especially during the second part of the stroke due to the high pressure inside the secondary chamber. It shows that a shock absorber modelled using ideal gas law is less stiff due to the lower pressure. The other chosen *EOS* used in the simulation predict more accurate results. Their force-stroke curves are almost on top of each other. Even van Der Waals *EOS* could be used, although according to literature it's accuracy is limited. [3].

4.2 Dynamic case

The dynamic test setup is based on a nitrogen actuator. It has a tank of highly pressurised nitrogen, which operates a cylinder that is attached to the end of the shock absorber. The other end is rigidly supported. With this setup, the shock absorber can be compressed rapidly.

In the simulation, the measured force, as a function of time, was given as an input to the model and is shown in fig. 5. Then the stroke rate and the stroke of the shock absorber was calculated. These were then compared to the measured values.

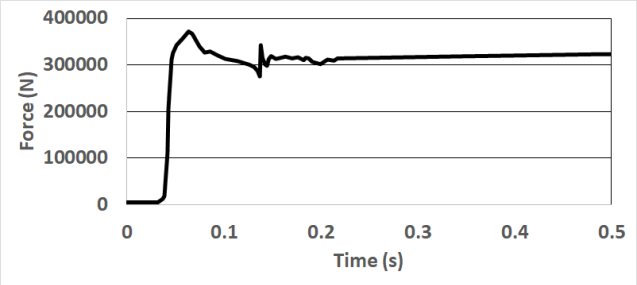

Figure 5: The given input force during the dynamical case.

Figure 6 shows the stroke during the dynamical compression. As expected, the maximum stroke that the ideal gas law produces is higher than the measured and maximum stroke produced by the other *EOS*. This is due to the lesser stiffness that was observed in the quasi-static compression. The other *EOS* behave similarly and produce a maximum stroke close to the measured.

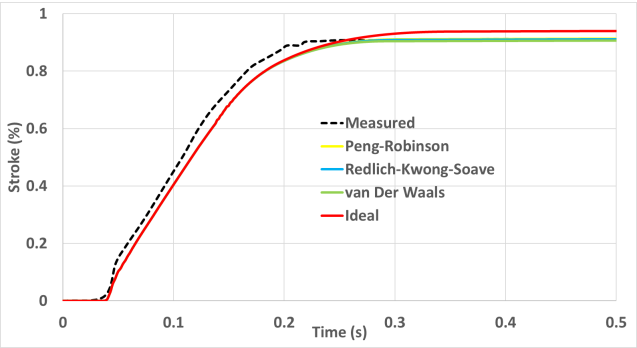

Figure 6: Stroke during the dynamical compression.

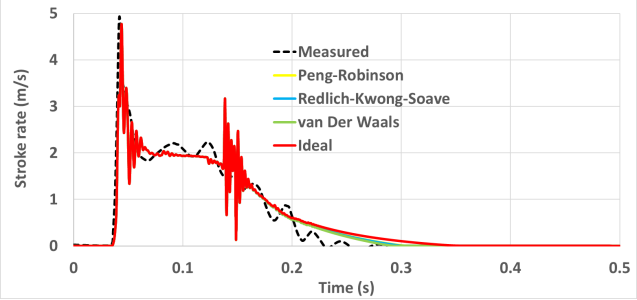

Figure 7: Stroke rate during the dynamical compression.

In addition, the stroke rate was modelled during dynamical compression. The results are shown in fig. 7. As the gas is responsible for the shock absorber stiffness, it has little effect on the shock absorber damping characteristics. Therefore, significant difference between the performance of different *EOS* cannot be observed. Ideal gas seems to reach zero stroke rate a bit slower than the other *EOS*. It is assumed that this is related to the larger maximum stroke observed.

In both cases the ideal gas law behaved poorly. Interestingly, the other *EOS* behaved similarly. However, the results were analyzed on a general level and more detailed analysis could show difference in the *EOS* behavior. In addition, according to literature, the Peng-Robinson is the most accurate *EOS* [6] and should be used.

5 Conclusion

In this paper, a model based on fundamental analytical mathematical equations of a two-stage naval fighter shock absorber was presented. In the model, gas volumes are modelled using general internal energy model. This requires derivatives of the gas density, which is solved from the chosen gas *equation of state* (EOS). Different *EOS* were used in the simulations. These were ideal gas, van der Waals, Redlich-Kwong-Soave, and Peng-Robinson. Two different cases were considered: quasi-static and dynamical compression. In the former case, the force of a given stroke was measured. In the latter the stroke rate and the stroke of a given force was measured. Using the model, both cases were simulated and the results from the simulation were compared to the measured data.

It was assumed that the pressure inside a naval fighter shock absorber rises so high that the accuracy of the ideal gas law is insufficient. This was seen in both cases. The ideal gas law predicted significantly lower reaction force during the quasi-static compression than the other three *EOS*. Especially, as the second chamber activates. Similarly, in the dynamic case, the shock absorber behaved less stiff, when the ideal gas law was used producing clearly higher maximum stroke.

Based on the aforementioned findings, it is suggested that the ideal gas law is not used when modelling fighter aircraft shock absorber. The other *EOS* were in good agreement with the measured values. However, the results were analyzed quite generally and a more detailed analysis is required. Also, there might be certain situations where the model differences can be clearly seen.

Designation	Denotation	Unit
α	Thermal diffusivity	m^2/s
α_P	Volumetric expansion coefficient	K^-1
β_T	Isothermal bulk modulus	Pa
ρ	Density	kg/m^3
ω	Acentric factor	
A	Flow area	m^2
A_{HP}	Secondary chamber area	m^2
A_L	Primary chamber area	m^2
A_{mp}	Metering pin cross-section	m^2
A_{ph}	Orifice support area	m^2
a	Constant	
b	Constant	
c_P	Specific heat	J/kgK
c_q	Flow coefficient	
Db	Damping coefficient	N/(ms)
dv	Relative velocity	m/s
E	Total energy	J
F_μ	Friction force	N
F_E	External force	N
F_{ext}	external force	N
F_{max}	higher limit contact force	N
F_{min}	lower limit contact force	N
F_S	Stiction force	N
F_{sa}	Force	N
F_V	Coulomb friction force	N
F_v	Coefficient of viscous friction	N/(m/s)
g	Gravitational acceleration	m/s^2
h	Specific enthalpy	J/kg
Kb	lower/higher limit stiffness	N/m
m	Mass	kg
m	Constant	
$\dot{m}$	Mass rate	kg/s
m_sa	Shock absorber mass	kg
Pd	penetration limit for full damping	m
P_c	Critical pressure	Pa
P_{sat}	Saturation pressure	Pa
p	Pressure	Pa
p_{HP}	Secondary chamber pressure	Pa
p_L	Primary chamber pressure	Pa
p_{ph}	Orifice support pressure	Pa
p_u	Orifice support pressure	Pa
Q	Exchanged heat	J
$\dot{Q}$	Heat exchange rate	W
R_{visc}	viscous friction coefficient	
r	Specific gas constant	J/kgK
T	Temperature	K
t	Time	s
T_c	Critical temperature	K
U	Internal energy	J
u	Specific internal energy	J/kg
V	Volume	m^3
V_{rel}	relative velocity	m/s
V_S	Stiction velocity	m/s
v	Specific volume	m^3/kg
W	Work	J
X_{max}	higher displacement limit	m
X_{min}	lower displacement limit	m
X_{ref}	Stroke length	m
X_{rel}	relative displacement	m

References

[1] Norman S Currey. *Landing gear design handbook*. Lockheed-Georgia Company, 1982.

[2] Benjamin Milwitzky and Francis E Cook. Analysis of landing-gear behavior. Technical report, NATIONAL AERONAUTICS AND SPACE ADMINISTRATION WASHINGTON DC, 1953.

[3] Yunus A Cengel and Michael A Boles. *Thermodynamics: an engineering approach*, volume 1000. 2002.

[4] James N Daniels. A method for landing gear modeling and simulation with experimental validation. 1996.

[5] Lucas G Horta, Robert H Daugherty, and Veloria J Martinson. Modeling and validation of a navy a6-intruder actively controlled landing gear system. 1999.

[6] Arttu Aleksi Heininen. Modelling and simulation of an aircraft main landing gear shock absorber. Master's thesis, 2015.

[7] Johannes Diderik Van der Waals. *Over de Continuiteit van den Gas-en Vloeistoftoestand*, volume 1. Sijthoff, 1873.

[8] Giorgio Soave. Equilibrium constants from a modified redlich-kwong equation of state. *Chemical engineering science*, 27(6):1197–1203, 1972.

[9] Otto Redlich and Joseph NS Kwong. On the thermodynamics of solutions. v. an equation of state. fugacities of gaseous solutions. *Chemical reviews*, 44(1):233–244, 1949.

[10] Ding-Yu Peng and Donald B Robinson. A new two-constant equation of state. *Industrial & Engineering Chemistry Fundamentals*, 15(1):59–64, 1976.

[11] William S Levine. *The Control Handbook (three volume set)*. CRC press, 2018.

[12] Dean Karnopp. Computer simulation of stick-slip friction in mechanical dynamic systems. *Journal of dynamic systems, measurement, and control*, 107(1):100–103, 1985.